Stability analysis for the flow in a dynamic wetting/dewetting gap

S. Strein[a] and **P. Ehrhard**[b]

[a]Institute for Nuclear and Energy Technologies
Forschungszentrum Karlsruhe
P.O. Box 3640, D-76021 Karlsruhe, Germany

[b]Fluid Mechanics, Biochemical and Chemical Engineering
University of Dortmund
Emil-Figge-Str. 68, D-44221 Dortmund, Germany

Presented at the 13th International Coating Science and Technology Symposium,
September 10-13, 2006, Denver, Colorado[1]

Dynamic wetting or dewetting is important in many industrial coating processes. The wetting of a solid with a liquid has great relevance e.g. in the production of photographical films, or in the production of LCD screens. In these manufacturing processes a high production rate and a good quality of the coating layers are demanded. The most common limitation in all coating processes is the wetting velocity. In 1959 Deryagin and Levi found experimentally that, given a sufficiently-high film velocity, coating failures crop up. In the case of coating failures, the dynamic contact line, where the three phases solid, liquid and gas merge, becomes unstable and transforms from a straight line into a saw-tooth shape. Additionally, air entrainment appears at the peaks of the saw-tooth triangles. As a consequence of such coating failures, the integrity of the coating layer is lost and the final product may be useless. Around an unstable dynamic contact line, the liquid and gas flows transform (from two-dimensional base flows) into three-dimensional flows. Various more recent experiments (Deryagin 1964, Perry 1967, Burley and Kennedy 1976, Blake and Ruschak 1979, Burley 1992) confirm that for coating velocities below the critical velocity the dynamic contact line remains straight, whereas at sufficiently-large velocities (above the critical velocity) the contact line develops a saw-tooth shape. The instability of the dynamic contact line is certainly linked to the stability of the flows on both sites of the wetting (dewetting) interface. Hence, it may be caused by the wetting liquid flow or by the dewetting gas flow, in which the dynamic contact angle approaches 180 degrees. For an accurate prediction of the critical coating velocity, therefore, it appears highly desirable to investigate the stability of the flows on either side of the free interface for this coating situation.

Currently, we focus within our stability analysis onto a wetting process, where a tape is (vertically) plunging into a large pool of liquid (cf. figure 1). In the convergent gap between the moving solid strip and the free interface a gas flow is present, which essentially removes the gas from the solid to allow for the liquid coating. The gas flow in this convergent gap is studied in the following stability analysis. In principle, there are two different types of gas flow possible; in

---

figure 1 these are sketched and termed type 1 and type 2.

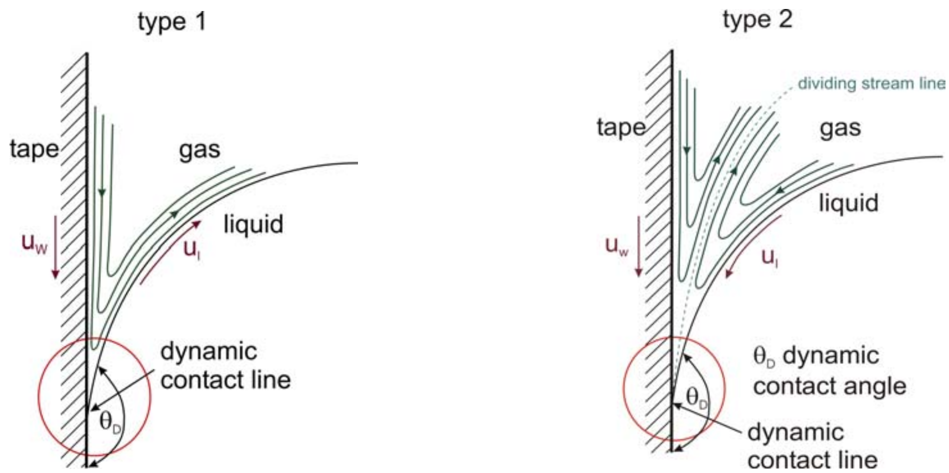

Fig. 1. Principle sketch of possible flows in the convergent gas gap.

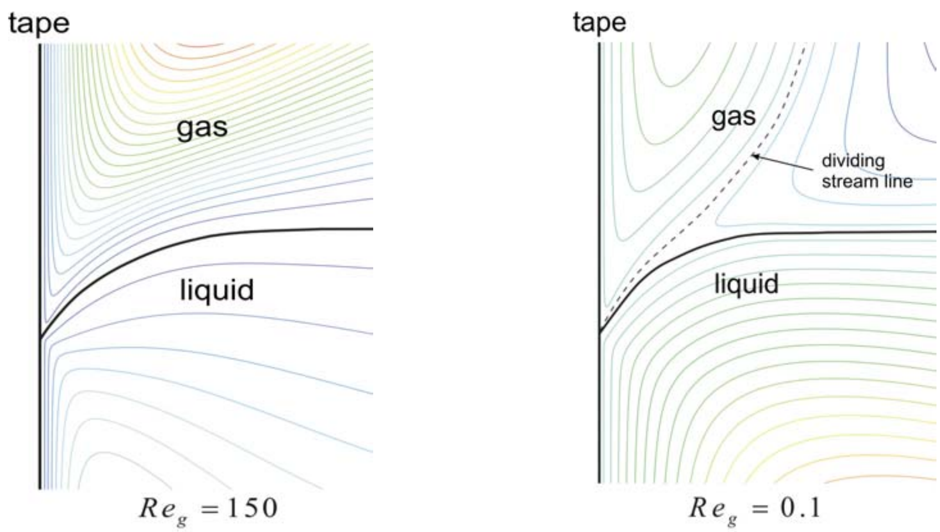

Fig. 2. FEM simulations for $Re_g=150$ and $Re_g=0.1$.

In both figures the tape moves with the wall velocity u_w into the pool of liquid. For type 1 the gas flow is directed out of the convergent gap along the free gas/liquid interface. For type 2 the flow is directed out of the convergent gap along a dividing stream line, while at the free gas/liquid interface the flow is directed into the gap (contrary to type 1). Experimental and numerical studies of the flows near the dynamic contact line (cf. Royon & Ehrhard 2001) show that, depending on the gas Reynolds number

$$Re_g = \frac{u_W r_0}{\nu_g},$$

and on the viscosity ratio μ_g/μ_l, one obtains the flow structures of type 1 or type 2 for a given contact angle Φ_D. r_0 denotes the (constant) radius of curvature, approximated for the free interface. Figure 2 illustrates the different flow patterns of type 1 and type 2 for liquid Reynolds numbers of $Re_g=150$ and $Re_g=0.1$, and for a constant viscosity ratio $\mu_g/\mu_l =0.017$, obtained from numerical (FEM) simulations. The parameters are taken from the system water/air, whereas the variation of the tape velocity allows to vary the Reynolds number. Figure 2 gives streamlines at a (constant) dynamic contact angle of $\Phi_D=150°$ for both cases.

For the stability analysis, we treat the gas as incompressible Newtonian fluid. The base flow in the wedge appears to be two-dimensional (plane) and steady, featuring the two basic patterns as discussed above. In a first step, the free interface is idealized as geometrically fixed and plane, featuring an opening angle of $\Phi_0=30°$. The kinematic boundary conditions are taken accurately at the moving tape and approximated at the free interface: for small μ_g/μ_l we can expect $U_l \rightarrow -U_w$ (type 2), for large μ_g/μ_l we can expect $U_l \rightarrow +U_w$ (type 1). The governing equations and boundary conditions are non-dimensionalized and formulated in cylindrical coordinates. This enables us to map e.g. the radial coordinate from the (infinite) interval $0 \le r \le \infty$ onto the finite interval $0 \le R \le R_\infty$. A principle sketch of both investigated wedge flows is given in figure 3.

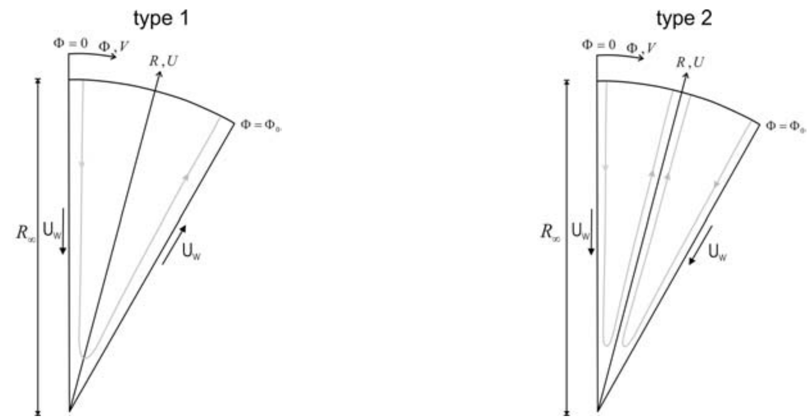

Fig. 3. Two basic patterns of wedge flows under investigation.

The base flows $\mathbf{V}_0$ (two-dimensional, steady) are subjected to small disturbances $\mathbf{V}'$ of amplitude ε, which are three-dimensional and time-dependent, i.e. we use

$$\mathbf{V} = \mathbf{V}_0(R,\Phi) + \varepsilon \mathbf{V}'(R,\Phi,\tau,Z).$$

For the perturbation analysis, the disturbance terms are modelled by Fourier series in Φ and by complex exponential functions in time τ and Z. Hence, we use

$$\mathbf{V}' = \sum_{k=1}^{N} A_k(R,\Phi)\exp(i(\omega\tau + aZ)), \quad \omega = \omega_{re} + i\omega_{im}, \quad k = 1,2,3,\ldots .$$

The above ansatz for the disturbances allows for periodic behaviour in Z and for periodic and damped/amplified behaviour in time. From the Fourier series in Φ we consider solely terms, which satisfy the kinematic boundary conditions for the disturbances, namely

$$\mathbf{V}'(0) = 0, \quad \mathbf{V}'(\Phi_0) = 0.$$

The perturbation ansatz is implemented into the time-dependent and three-dimensional Navier-Stokes equations, and a Galerkin method is applied to integrate along Φ within the range $0 \le \Phi \le \Phi_0$. Hence, we arrive at a system of linear, homogenous ordinary differential equations for the Fourier coefficients $B_k(R)$, governing the radial behaviour of the perturbations. The two-point boundary value problem for the coefficients $B_k(R)$ can be solved numerically, and for each eigen value $\omega_{im,k}$ both the differential equations and the boundary conditions at $R = 0$ and $R = R_\infty$ can be fulfilled.

For both types of flows figure 4 shows at a dynamic contact angle of *150 degrees* (opening angle *30 degrees*) the stability results. The first few eigen values $\omega_{im,k}$ are plotted against wave number a for different modes k and (modified) Reynolds numbers $Re = u_w r_\infty \Phi_0/\nu_g$. For the wave number

$a \rightarrow 0$, two-dimensional and time-dependent disturbances are present, while for $a \geq 0$ spatially-periodic (in Z) and time-dependent disturbances are considered. As conclusion from the two-dimensional case ($a = 0$) we find only eigen values $\omega_{im,k} > 0$, $\omega_{re,k} = 0$, ensuring all disturbances to be damped in time in an exponential fashion. Moreover, with increasing Reynolds numbers the eigen values approach zero, clarifying that increasing Reynolds numbers tend to destabilize the system, i.e. larger Re lead to weaker damping of the disturbances. For the three-dimensional time-dependent case, we find with increasing wave numbers a increasing eigen values $\omega_{im,k}$. This means that (at constant Reynolds number) shorter wave lengths (in Z) are in general more stable than infinite wave lengths ($a \rightarrow 0$). Finally, all higher modes (cf. second mode, etc.) give larger eigen values $\omega_{im,k}$ compared to the first mode. In conclusion, the first mode appears to be the most critical mode. The base flow in the convergent gap with straight (approximated) boundaries, in summary, appears to be stable against small disturbances of all kinds.

Further, we have conducted purely-numerical (three-dimensional, time-dependent, FEM) disturbance investigations, which recover the analytical eigen values for both types of flow, provided that small perturbations are introduced. Larger perturbations, which can be likewise introduced in such numerical studies, in all cases have been found to be damped in time, however, at slightly different exponential behaviour. These simulations ensure that (i) the analytical stability analysis has captured the dominant modes and that (ii) qualitatively-similar behaviour is present if finite-amplitude disturbances are introduced. In our present studies, we extend the idealized base flows towards a more realistic geometry and towards more realistic (stress) boundary conditions of/at the free interface. In particular, the free interface has a defined (and constant) radius of curvature, introducing a secondary length scale.

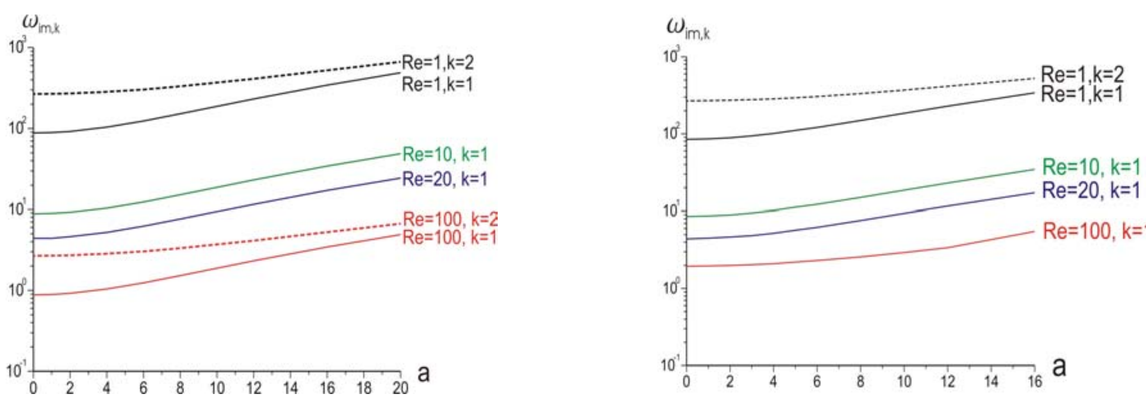

Fig. 4. Leading eigen values for wedge flows of type 1 and type 2.

References

Blake, T., Ruschak, K.: 1979, A maximum speed of wetting, *Nature* **282**, 489-491.

Burley, R.:1992, Air entrainment and the limits of coatability, *JOCCA* **5**, 192-202.

Burley, R., Kennedy, B.: 1976, An experimental study of air entrainment at a solid/liquid/gas interface, *Chemical Engineering Science* **31**, 901-911.

Deryagin, B. M., Levi, S. M.: 1964, Film coating theory, *Focal Press*, **137**, 190.

Perry, R.: 1967, Fluid mechanics of entrainment through liquid-liquid and liquid-solid junctures, *PhDthesis*, University of Minnesota, Minneapolis.

Royon, A., Ehrhard, P.: 2001, Strömungsstruktur nahe einer bewegte Kontaktlinie, *Technical Report FZKA 6627*, Forschungszentrum Karlsruhe.